Publication in the journal 'Oxidation of Metals' (Peer-reviewed)

High Temperature Oxidation Behavior of Refractory High Entropy Alloys: Effect of Alloy Composition

Bronislava Gorr[a], Franz Müller[a], Maria Azim[a], Hans-Jürgen Christ[a], Torsten Müller[b], Hans Chen[c], Alexander Kauffmann[c], Martin Heilmaier[c]

[a]*Institut für Werkstofftechnik, Universität Siegen, Paul-Bonatz Str.9-11, 57068 Siegen, GERMANY*
[b]*Institut für Bau- und Werkstoffchemie, Paul-Bonatz Str.9-11, 57068 Siegen, GERMANY*
[b]*Institut für Angewandte Materialien-Werkstoffkunde, Karlsruhe Institute of Technology, Engelbert-Arnold-Str. 4, 76131 Karlsruhe, GERMANY*

gorr@ifwt.mb.uni-siegen.de;franz.mueller@student.uni-siegen.de;maria.azim@uni-siegen.de; christ@ifwt.mb.uni-siegen.de; t.mueller@chemie.uni-siegen.de;hans.chen@kit.edu; alexander.kauffmann@kit.edu; martin.heilmaier@kit.edu

Abstract. The high temperature oxidation behavior of a new family of refractory high entropy alloys (HEAs) with compositions of W-Mo-Cr-Ti-Al, Nb-Mo-Cr-Ti-Al and Ta-Mo-Cr-Ti-Al was studied at 1000°C and 1100°C. Based on these equimolar starting compositions, the main incentive of this study was to select the most promising alloy system whose properties may then be successively improved. Despite the high amount of refractory elements, all HEAs studied here showed good oxidation resistance at least during 48h of air exposure at 1000°C and 1100°C. Moderate values of mass gain and complex oxidation kinetics were observed for the W- and Nb-containing HEAs. These alloys formed inhomogeneous oxide scales possessing regions with thick and porous layers as well as areas revealing quite thin oxide scales due to the formation of discontinuous Cr- and Al-rich scales. The most promising behavior, though, was shown by the alloy Ta-Mo-Cr-Ti-Al which followed the parabolic rate law for oxide growth due to the formation of a thin and compact Al-rich layer.

Keywords: high entropy alloys, refractory metals, oxidation kinetics, oxide scale morphology, oxide evaporation

INTRODUCTION

Alloys based on refractory metals are potentially very attractive for high temperature applications primarily because of their high melting points [1]. Extended explorations of refractory-based materials aiming at a practical use of these materials in ambient environment at high temperatures were undertaken in the fifties and sixties of the 20th century [2]. However, the commercial implementation of these alloys as structural materials has largely been prohibited since they suffered from severe drawbacks such as insufficient ductility at low temperatures and poor oxidation resistance. Currently, refractory elements, such as Mo, W, Re, are added in only moderate concentrations to conventional high temperature materials such as Fe- and Ni-based alloys, to enhance their strength [3]. Nevertheless, some refractory-based alloy systems are still intensively investigated and their properties have been significantly improved. For example, Bewlay et al. reported on the excellent balance between room- and high-temperature mechanical properties and oxidation behavior of advanced Nb-based composites consisting of a Nb-

based solid-solution with Nb_3Si and Nb_5Si_3-type silicides [4]. Significant improvements in high temperature oxidation behavior of Mo-based alloys have been recently achieved due to macroalloying with Ti [5].

In the last years, so-called high-entropy alloys and particularly refractory HEAs have attracted steadily increasing attention among scientist worldwide [6-9]. In HEAs, elements possess equal or nearly-equal concentrations. From the thermodynamic point of view, such alloys exhibit high entropy of mixing; the formation of simple solid-solution is, therefore, favored, while the appearance of intermetallic phases is suppressed because of their ordered structure and, consequently, much lower entropy of mixing [6]. Some new refractory HEAs show extremely high strength at elevated temperature and have, thus, been considered as perspective materials for high temperature application [7]. Recently, a new equimolar refractory alloy system X-Mo-Cr-Ti-Al was proposed by Gorr et al. [10]. Extensive microstructural analyses were carried out for W-Mo-Cr-Ti-Al and Nb-Mo-Cr-Ti-Al alloys, and mechanical properties at room and elevated temperatures were investigated for the Nb-containing alloy [10-12]. The oxidation resistance has been studied in detail for the alloy Nb-Mo-Cr-Ti-Al [13], while oxidation behavior of the W-containing HEA was only briefly assessed [10]. Novel experimental results on the oxidation behavior of the alloy Ta-Mo-Cr-Ti-Al have meanwhile been obtained.

Hence, this paper represents a comparative study of a refractory based HEA family of type X-Mo-Cr-Ti-Al (with X=W, Nb, Ta) in terms of high temperature oxidation resistance aiming at selecting the most promising equimolar alloy systems whose properties might be further improved by microalloying in future work.

EXPERIMENTAL PROCEDURES

All alloys were produced from elemental bulk materials by arc-melting in ~0.6 atm of argon (arc-melter AM 0.5 by Edmund Bühler GmbH). The purities of the starting materials Ta, Mo, Nb, Al were all 99.9%, W was available in 99.96% purity, whereas Cr and Ti had a purity of only 99% and 99.8%, respectively. In the alloys, nitrogen impurities were found to be below the detection limit, oxygen content was measured being between 50 and 100 wt. ppm. The prepared buttons were flipped over and remelted more than five times in a water-chilled copper mold to facilitate alloy homogenization. Oxidation tests of the alloy W-Mo-Cr-Ti-Al were performed on samples in the as-cast condition, while Nb- and Ta-containing alloys were heat-treated (1200°C for 20h) before oxidation. Thermogravimetric experiments were carried out in static laboratory air at 1000°C and 1100°C. Detailed sample preparation procedures as well as detailded description of oxidation tests can be found elsewhere [13]. The oxide scale morphology was analyzed by means of a FIB-SEM DualBeam system of type FEI Helios Nanolab 600 equipped with an energy dispersive X-ray (EDX) detector. To analyze the composition of oxides formed on the alloys, X-ray diffraction (XRD) measurements were carried out using the X'Pert Pro MPD diffractometer operating in Bragg-Brentano geometry. Oxide scales formed on W- and Nb-containing alloys were removed from the oxidized samples, powdered into particle sizes smaller than 40 µm and analyzed as described in Ref. [13]. Since the oxide scales formed on the alloy Ta-Mo-Cr-Ti-Al were extremely thin, XRD measurements were conducted directly on oxidized samples, i. e. without removing the oxide layers. To support experimental observation and to get a more fundamental knowledge of the alloy systems, thermodynamic calculations were carried out using the software FactSage V6.4 in conjunction with a commercial database.

RESULTS

Figure 1 compares oxidation kinetics of the alloys W-Mo-Cr-Ti-Al, Nb-Mo-Cr-Ti-Al and Ta-Mo-Cr-Ti-Al at 1000°C and 1100°C. The alloy Nb-Mo-Cr-Ti-Al exhibits a relatively high mass gain at both temperatures. At 1000°C, the thermogravimetric curve obviously obeys the linear rate law, while the curve at 1100°C shows clearly decelerating oxidation kinetics. The oxidation kinetics of the alloy W-Mo-Cr-Ti-Al obeys the parabolic rate law for approximately 40h at 1000°C. After that, the oxidation behavior changes towards higher oxidation rates following the linear rate law. An effect similar to breakaway oxidation takes place indicating a change in the scale structure towards formation of thick, porous and non-protective scales. As opposed to this, the oxidation curves of the alloy Ta-Mo-Cr-Ti-Al follows the parabolic rate law during the full 48h of air exposure at both temperatures indicating the formation of a highly protective oxide scales.

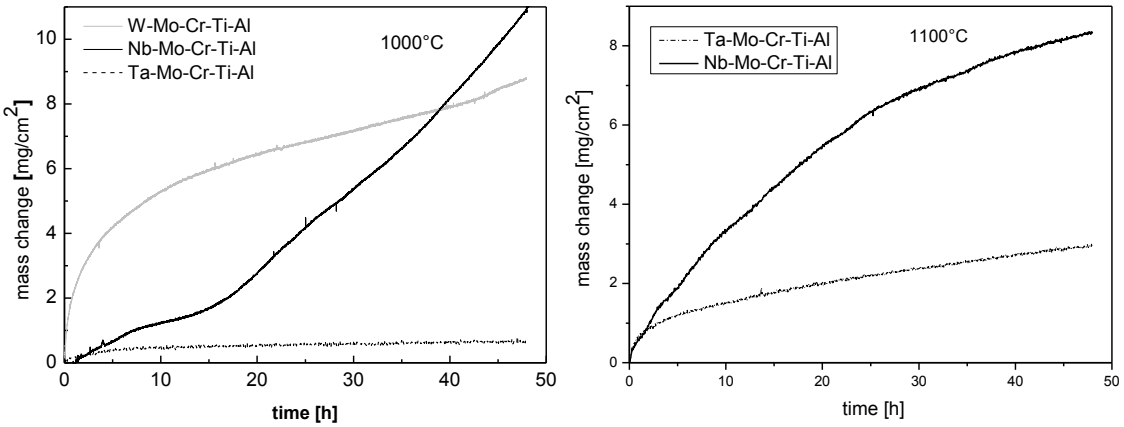

(a) (b)

FIGURE 1. Thermogravimetric curves of HEAs W-Mo-Cr-Ti-Al, Nb-Mo-Cr-Ti-Al and Ta-Mo-Cr-Ti-Al at (a) 1000°C and (b) 1100°C

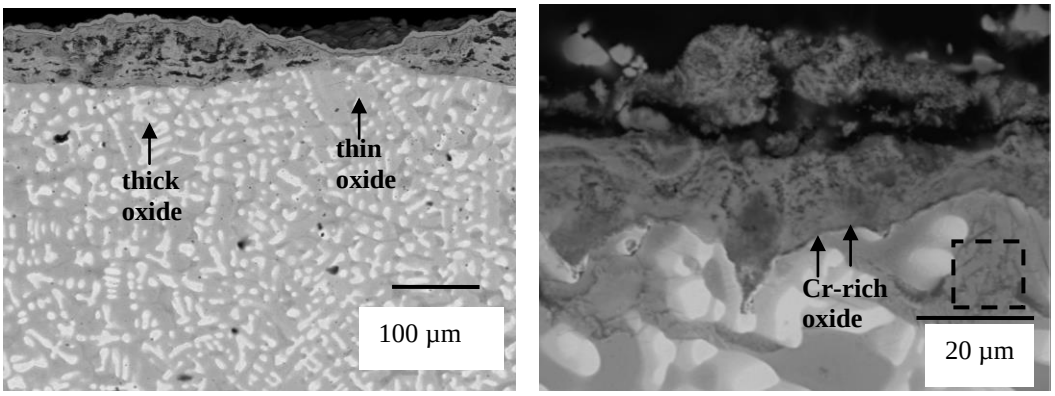

(a) (b)

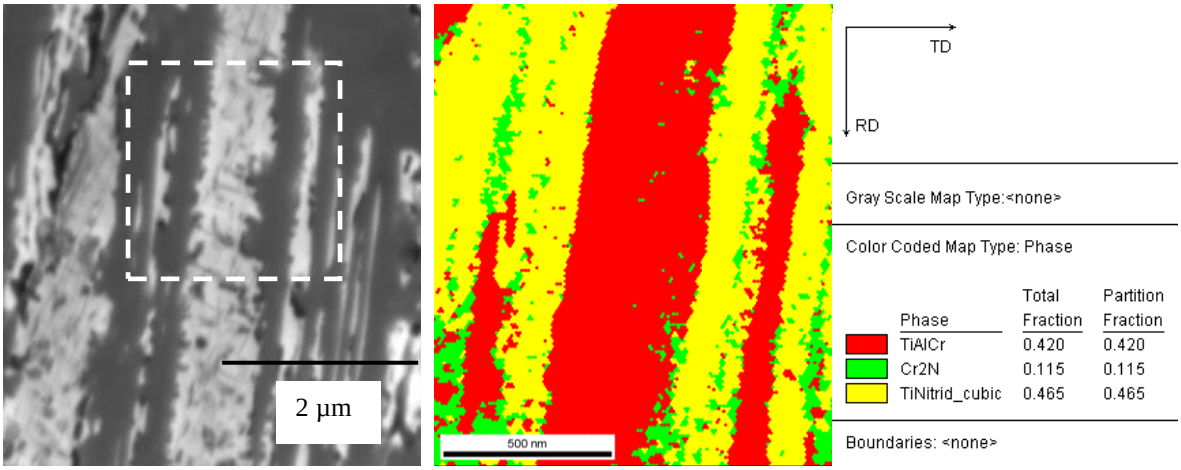

(c)

FIGURE 2. Corrosion products formed on the alloy W-Mo-Cr-Ti-Al after 48h of oxidation at 1000°C; (a) cross-section (BSE-mode) of the oxidized sample, (b) high magnification of the thin oxide scale region and (c) formation of Cr_2N and TiN as internal precipitates

Figures 2 (a) and (b) show the non-uniform oxide scale formed on the alloy W-Mo-Cr-Ti-Al after 48h of oxidation at 1000°C. Two different kinds of oxide morphology can be observed: (i) thick (up to ~ 180µm) and porous oxide mixture and (ii) a relatively thin (up to ~ 20µm) and compact oxide layer. EDX analysis (not shown here) of these two distinctive regions revealed that Ti, Al, Cr, W and O are nearly homogeneously distributed in the thick oxide, while a discontinuous layer of a Cr-rich oxide was identified at the interface oxide/substrate in the case of the thin oxide layer [10]. Interestingly, enrichment of Mo was found at the interface oxide/substrate underneath the thin oxide layers. A closer look at this interface (s. Fig. 2 (b)) reveals some additional particular features: (i) the W- and Mo-rich dendrites (bright phase in the BSE contrast) possess a poorer oxidation resistance compared to the matrix and (ii) underneath the relatively thin oxide layer, internally formed precipitates (marked in Fig. 2(b)) are observed. To determine the nature of these precipitates, EBSD analysis was performed. Figure 2 (c) shows that these precipitates are rich in Ti, Al and Cr. Two types of nitrides were identified, namely Cr_2N and TiN.

To identify the nature of the corrosion products formed on the alloy W-Mo-Cr-Ti-Al depending on the oxidation time, the oxide scales were removed from the samples oxidized 8h, 24h and 48h in air at 1000°C, powdered and analyzed using XRD. The results of this analysis reveal that three types of lattice structures were present, namely rutile, corundum and aluminium tungstate. Rutile was detected after all oxidation times, and can clearly be related to the formation of TiO_2 as confirmed by the EDX analysis. With respect to corundum, two oxides that can form in this alloy during oxidation, i.e. Al_2O_3 and Cr_2O_3, possess this crystal structure. Bondioli et al. reported that above 950°C a solid solution exists between alumina-rich and chromia-rich crystalline phases [14]. In the alloy W-Mo-Cr-Ti-Al, corundum was detected after 8h and 48h of oxidation, while after 24h and 48h the formation of aluminium tungstate $Al_2(WO_4)_3$ that results from the reaction of Al_2O_3 with WO_3 was confirmed as reported by other authors as well [15]. According to Waring, this compound may form in a wide concentration range and remains stable at temperatures up to 1200°C [16]. As aluminium tungstate was only detected after prolonged oxidation time in the alloy W-Mo-Cr-Ti-Al, the kinetics of $Al_2(WO_4)_3$ formation is obviously slow.

The detailed description of the microstructure analyses of the oxide scales formed on the alloy Nb-Mo-Cr-Ti-Al can be found elsewhere [13]. In summary, oxide scales formed on this alloy after air exposure at 1000°C and 1100°C are rather inhomogeneous exhibiting regions with thick layers as well as areas showing quite thin oxide layers due to the formation of discontinuous chromium- and aluminium-rich scales (see. Fig. 3). XRD analysis revealed that two crystal structures, rutile and corundum are present as corrosion products in the outer oxide scale after 24h and 48h air exposure at 1000°C. After short oxidation time, i.e. 8h, anatase, TiO_2 in the tetragonal structure, was additionally found in the oxide scale. Underneath the thin layers, Mo enrichments were identified using EDX. In contrast to the W-containing alloy, a thick zone (up to 30 µm) of internal corrosion was observed beneath the thin oxide scales [13].

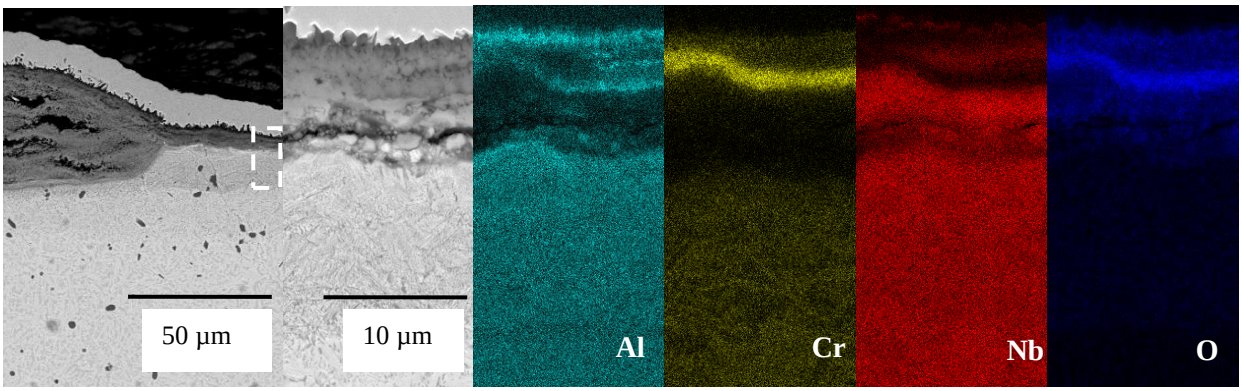

FIGURE 3. Oxide scales formed on the alloy Nb-Mo-Cr-Ti-Al after air exposure at 1000°C for 48h; the white box on the farthest left micrograph indicates the area chosen for EDX analysis (right color-coded micrographs)

As opposed to the W- and Nb-containing alloys, a homogeneously thin (up to 7µm) and continuous oxide scale was observed on the alloy Ta-Mo-Cr-Ti-Al after 48h of oxidation at 1000°C. Figure 4 shows the microstructure of the oxide scale: beneath the coarse Ti oxide particles, an extremely thin Al oxide layer can be identified that obviously provides a high oxidation resistance (see also the weight gain curves in Fig. 1). Underneath the Al oxide

layer, Cr, Ti and Nb were detected using EDX. However, a pronounced zone (up to 15µm) of internal corrosion was also identified. Results of the XRD analysis reveal that TiO_2, Al_2O_3, Cr_2O_3 and probably $CrTaO_4$ are present in the oxide scale after 48h of air exposure at 1000°C, while some Cr_2N seems to have been internally precipitated. It should, however, be mentioned that these microstructural investigations of oxide scales and internal precipitates are of preliminary nature and need to be intensified in future work.

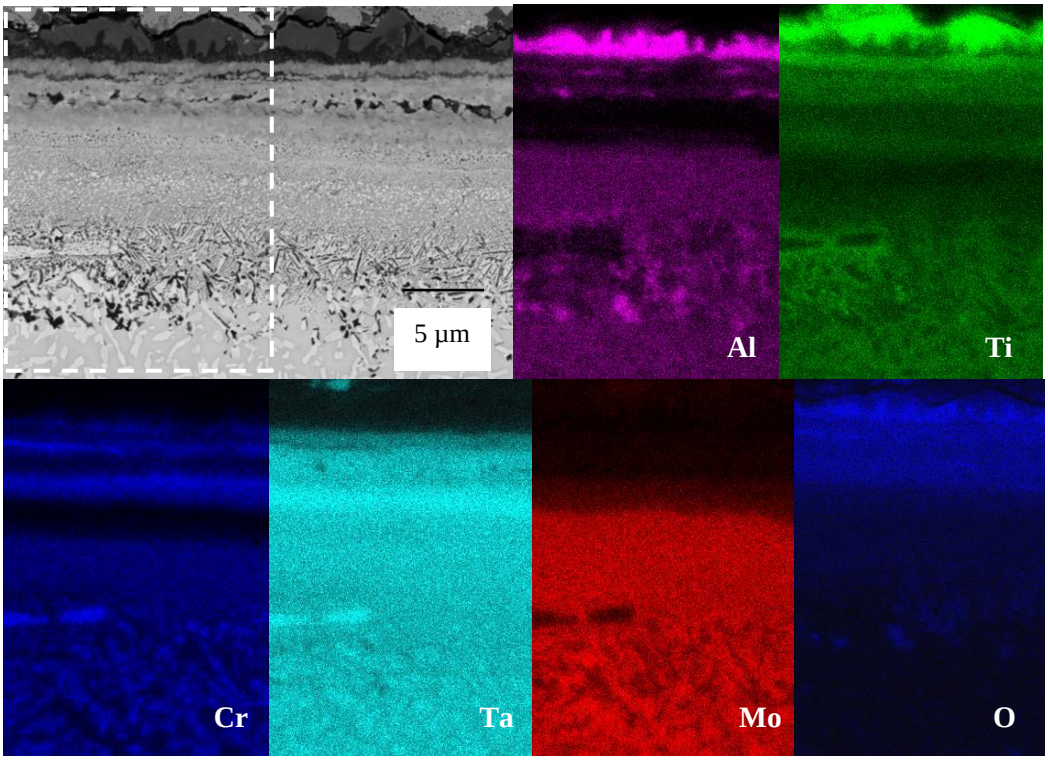

FIGURE 4. Oxide scale formed on the alloy Ta-Mo-Cr-Ti-Al after air exposure at 1000°C for 48h; again the white box on the left upper micrograph indicates the area chosen for EDX analysis

DISCUSSION

Considering the high amount of refractory elements in all HEAs studied, it can be stated that the alloys show acceptable or even very good oxidation resistance at least during 48h of air exposure at 1000°C and 1100°C. Figure 5(a) compares the oxidation rates of HEAs investigated in this study with those of some commercial Ni-based superalloys and alloys containing the relevant refractory elements such as W, Nb and Ta. Figure 5(a) reveals that our HEAs show, in general, superior oxidation resistance compared to most of the refractory-based alloys and yields, therefore, a high potential in terms of high temperature corrosion resistance. However, the oxidation resistance of Ni-based alloys is clearly better as compared to those of the W- and Nb-containing HEAs, although the alloy Ta-Mo-Cr-Ti-Al shows comparatively good values of oxidation rates at 1000°C and 1100°C.

The dominant contribution to the mass gain during oxidation can obviously be attributed to the oxygen uptake as relatively thick oxide scales were observed on the alloys W-Mo-Cr-Ti-Al and Nb-Mo-Cr-Ti-Al. It is well-known that pure chromia and alumina possess very low oxidation rates. Refractory metals, however, exhibit very poor oxidation resistance. In order to understand the role of refractory elements in the alloys, oxidation rates of the pure refractory metals W, Mo, Nb, Ta and Cr at temperatures between 800°C and 1100°C are summarized in Fig. 5(b). Apparently, oxidation rates of W, Mo, Nb and Ta are several order of magnitude higher compared to, for example, that of Cr. It is well-known that pure Mo forms gaseous oxides above 800°C that evaporate extremely fast [17]. By contrast, W, Nb and Ta oxidize forming solid oxides at temperatures of interest. In fact, W also forms gaseous WO_3, However, Gulbransen et al. observed severe evaporation of tungsten trioxide only at temperatures well above

1150°C [18]. Figure 5(b) clearly shows that W yields the highest oxidation rate at temperatures between 900°C and 1100°C. This seems to be the probable reason for the high mass gain of the alloy W-Mo-Cr-Ti-Al during air exposure at 1000°C, especially of the dendritic regions that have a very high W content (see Fig. 2(b)). In the temperature range between 900°C and 1100°C, pure Ta and Nb possess similar oxidation resistance, where Ta exhibits only a slightly lower oxidation rate as compared to Nb.

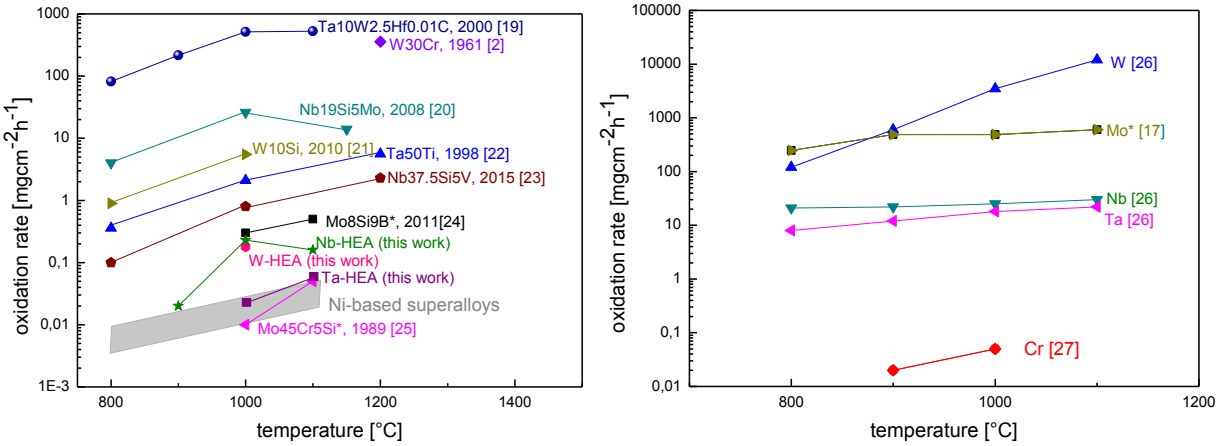

FIGURE 5. (a) oxidation rates of Ni-based superalloys, some refractory alloys and HEAs investigated in this study and (b) oxidation rates of pure refractory metals; oxidation rates of Mo and alloys marked with* are negative

Weight gain curves of HEAs observed during oxidation in air can be ascribed not only to oxygen but also to nitrogen uptake as nitrides were experimentally identified in the zones of internal corrosion observed in all alloys. It should be pointed out that the zone of internal corrosion is most pronounced for the Nb-containing alloy, while the thinnest one was observed in the alloy W-Mo-Cr-Ti-Al. In order to understand this experimental finding and to assess the effect of each element in the alloy W-Mo-Cr-Al-Ti on the ability of the metallic matrix to dissolve nitrogen, the mole fraction of dissolved nitrogen in the BCC phase was calculated as a function of alloy element concentrations (Fig. 6). The concentration of one element was changed, while the contents of the other elements were kept equal. It seems that W in this alloy plays a crucial role in terms of nitrogen solubility decreasing the amount of dissolved nitrogen in the BCC phase extremely efficiently. It can, therefore, be concluded that decreased concentration of W may lead to the enhanced formation of various nitrides in the considered alloy system. In contrary, Cr additions do not influence the nitrogen solubility notably. Further, decreasing the Ti content up to 15 at.% may cause substantial lowering the nitrogen solubility in the alloy (see Fig. 6). Ti concentrations below this critical value, though, do not affect the nitrogen solubility significantly.

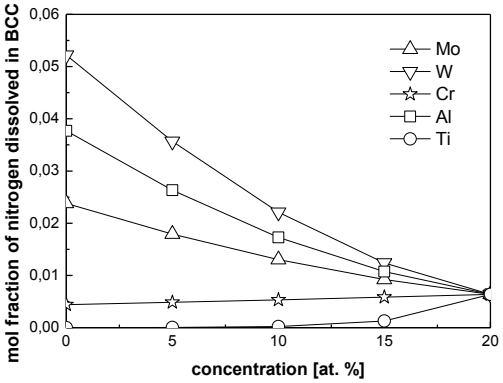

FIGURE 6. Nitrogen dissolved in the the BCC phase of the alloy W-Mo-Cr-Ti-Al versus element concentration

Table 1 summarizes literature values of oxygen and nitrogen solubility in those elements being present in alloys studied. It is apparent that W, Mo, Cr and Al do not support gas solubility in HEAs, while Nb, Ta and Ti may contribute to oxygen and/or nitrogen solubility in the alloys. The extremely low values of oxygen and nitrogen solubility in pure W support the above suggestion that W seems to counteract the gas solubility. Comparing the corresponding values of oxygen and nitrogen solubility in pure W, Ta and Nb, it can be concluded that Nb-containing alloys, as compared to Ta- and especially W-containing ones, may be intrinsically prone to dissolve notable amounts of oxygen and nitrogen which cause substantial internal corrosion. Taking into account that all alloys in this study contain the same concentration of Ti, which possesses an extremely high ability to dissolve gases, and considering the rather thin zone of internal corrosion in the W-containing HEA, it seems that the deleterious effect of Ti in terms of gas solubility may largely be excluded.

TABLE 1. oxygen and nitrogen solubility in pure elements

Elements	**W**	**Nb**	**Ta**	**Mo**	**α-Ti**	**Cr**	**Al**
O solubility, at.%	0.03 [28]	2.5 [29]	3 [30]	0.03 [28]	33 [31]	0.0006 [28]	~0
N solubility	0.4 ppm [32]	14.5 at.% [33]	4 at.% [34]	20 ppm [35]	17 at.% [36]	0.08 at.% [28]	~0

Results of the XRD measurements are useful to indicate tendencies in the oxidation behavior of HEAs. Comparing the development of oxides formed on the alloys W-Mo-Cr-Ti-Al and Nb-Mo-Cr-Ti-Al, it becomes clear that despite the obvious parabolic behavior for a certain period and a slightly less mass gain after 48h oxidation at 1000°C, the alloy W-Mo-Cr-Ti-Al shows a significantly lower potential in terms of high temperature oxidation resistance. This is because of the disadvantageous reaction between Al_2O_3 and WO_3 that results in the formation of aluminium tungstate $Al_2(WO_4)_3$. Obviously, this reaction reduces the probability to form a continuous and protective Al_2O_3 layer. Although corundum could be detected in the oxide scale of the W-containing alloy after 48h of oxidation at 1000°C, it is likely attributed to Cr_2O_3 rather than to Al_2O_3 formation as a thin and discontinuous Cr-rich oxide layer was identified at the interface oxide/substrate. Despite the high oxidation rates during oxidation, the alloy Nb-Mo-Cr-Ti-Al shows a higher potential to form a protective alumina scale. The formation of a protective alumina in this alloy can successfully be facilitated by higher temperatures, prolonged oxidation times and microalloying, e.g. with Si [13]. The alloy Ta-Mo-Cr-Ti-Al forms a protective alumina scale after 48h of air exposure at 1000°C and 1100°C and seems to be the most promising system. The mechanisms of alumina scale formation, the protective properties of $CrTaO_4$, as well as the role of TiO_2 in oxidation mechanisms are, though, not clear and should be thoroughly studied in future work.

CONCLUSIONS

The comparative study of oxidation resistance of three HEAs at 1000°C and 1100°C revealed that despite a period of parabolic oxidation, the alloy W-Mo-Cr-Ti-Al possesses the lowest ability to form a protective alumina scale because of the disadvantageous reaction between Al_2O_3 and WO_3 that results in the formation of fast growing aluminium tungstate $Al_2(WO_4)_3$. Even though the HEA Nb-Mo-Cr-Ti-Al exhibits rather high oxidation rates, this alloy possesses a clear potential to form an alumina scale. However, this alloy system shows a particular tendency to dissolve high amounts of oxygen and nitrogen as a thick zone of internal corrosion was observed. The alloy Ta-Mo-Cr-Ti-Al obviously exhibits a superior oxidation resistance compared to its counterparts. Due to the formation of a thin and dense alumina scale underneath the rutile layer, oxidation kinetics obeys the parabolic rate law resulting in extremely low mass gain. Apparently, the oxidation mechanisms of this alloy need to be investigated in more detail to exploit its full potential.

ACKNOWLEDGMENTS

The financial support by Deutsche Forschungsgemeinschaft (DFG) is gratefully acknowledged.

REFERENCES

1. J.H. Perepezko, *Science*, **326**, 1068 (2009).
2. R. Syre, Niobium, Molybdenum, tantalum and tungsten: A summary of their properties with recommendation for research and development, North Atlantic Treaty Organization, Advisory group for aeronautical research and development, 1961.
3. L. Huang, X.F. Sun, H.R. Guang, Z.Q. Hu, *Oxidation of Metals* **65**, 391 (2006).
4. B.P. Bewlay, MR. Jackson and H.A. Lipsitt, *Metallurgical and Materials Transactions A*, **27A**, 3801 (1996).
5. M. Azim, D. Schliephake, C. Hochmuth, B. Gorr, H.-J. Christ, U. Glatzel, M. Heilmaier, *JOM*, **57**, 2621 (2015).
6. J.W. Yeh, Y.L. Chen, S.J. Lin, S.K. Chen, *Materials Science Forum*, **560**, 1 (2007).
7. O.N. Senkov, C. Woodward, D.B. Miracle, *JOM*, **66**, 2030 (2014).
8. O.N. Senkov, S.V. Senkova, D.M. Dimiduk, C. Woodward, D.B. Miracle, *Journal of Materials Science*, **47**, 6522 (2012).
9. C.M. Liu, H.M. Wang, S.Q. Zhang, H.B. Tang, A.L. Zhang, *Journal of Alloys and Compounds*, **583**, 162 (2014).
10. B. Gorr, M. Azim, H.-J. Christ, T. Mueller, D. Schliephake, M. Heilmaier, *Journal of Alloys and Compounds*, **624**, 270 (2015).
11. H. Chen, A. Kauffmann, B. Gorr, D. Schliephake, C. Seemüller, J.N. Wagner, H.-J. Christ, M. Heilmaier, *Journal of Alloys and Compounds*, **661**, 206 (2015).
12. B. Gorr, M. Azim, H.-J. Christ, H. Chen, D.V. Szabo, A. Kauffmann, M. Heilmaier, *Metallurgical and Materials Transactions A*, **47A**, 961 (2016).
13. B. Gorr, F. Mueller, H.-J. Christ, T. Mueller, H. Chen, A. Kauffmann, M. Heilmaier, *Journal of Alloys and Compounds*, submitted.
14. F. Bondioli, A.M. Ferrari, C. Leonelli, Manfredini, L. Linati, P. Musterelli, *Journal of the American Ceramic Society*, **83**, 2036 (2000)
15. S. Matthews, F. Taliana, B. James, *Surface &Coatings Technology*, **212**, 109 (2012).
16. J.L. Waring, *Journal of the American Ceramic Society – Discussion and Notes*, **48**, 493 (1965).
17. E.A. Gulbransen, K.F. Andrew, F.A. Brassant, *Journal of the Electrochemical Society*, **110**, 952 (1963).
18. E.A. Gulbransen, K.F.Andrew, F.A. Brassant, *Journal of the Electrochemical Society*, **111**, 103 (1961).
19. G.R. Smolik, D. A. Petti, J.P. Sharpe, S.T. Schuetz, Report INEEL/EXT-2000-01455, 2000.
20. K. Chattopadhyay, R. Mitra, K.K. Ray, *Metallurgical and Materials Transactions A*, **39A**, 577 (2008).
21. T. Weissgaerber, B. Kloeden, B. Kieback, PM2010 World Congress- Tungsten & Molibdenum Alloys.
22. Y. Park, D.P. Butt, *Oxidation of Metals*, **51**, 383 (1999).
23. F. Gang, K. Klinski-Wetzel, J.N. Wagner, M. Heilmaier, *Oxidation of Metals*, **83**, 119 (2015).
24. S. Burk, B. Gorr, M. Krüger, M. Heilmaier, H.-J. Christ, *JOM*, **63**, 32 (2011).
25. D.B. Lee, G. Simkovich, *Oxidation of Metals*, **31**, 265 (1989).
26. N.M. Geyer, Protection of refractory metals against atmospheric environments, http://contrails.iit.edu/DigitalCollection/1961/ASDTR61-322article07.pdf. Assessed 1.03.2016
27. I. Murris, Y.P. Jacob, V.A.C. Haanappel, M.F. Stroosnijder, *Oxidation of Metals*, **55**, 307 (2001).
28. W.D. Klopp, *Recent developments in Chromium and Chromium alloys*, NASA-report TM X-1867, 1969.
29. R.P. Elliot, *Transaction of the ASM*, **52**, 900 (1960).
30. H. Jehn, E. Olzi, *Journal of the less Common Metals*, **27**, 297 (1972).
31. J.L. Murray, H.A. Wriedt, *Journal of Phase Equilibria*, **8**, 148 (1987).
32. R.L. Wagner, *Metallurgical Transactions*, **1**, 3365 (1970).
33. A. Taylor, Research for solubility of interstitials in columbium Part III. A study of columbium-rich alloys in the ternary systems Cb-Mo-O, Cb-Mo-N and Cb-Mo-C, Technical report, Westinghouse Research Labs Pittsburgh, 1966.
34. F.E. Bacon and P.M. Moanfeldt, Reaction with common gases, Columbium and Tantalum, John Wiley and Sons, New York, 1963.
35. D.E. Weaver, The diffusivity and solubility of nitrogen in molybdenum and trapping of nitrogen by carbon in molybdenum, PhD. Thesis, Lawrence Livermore Laboratory, University of California, 1972.
36. B. Holmberg, *Acta Chemica Scandinavica*, **16**, 1255 (1992).